Physics-based preconditioners for large-scale subsurface flow simulation.

Kees Vuik [1], Gabriela B. Diaz Cortes [1], Jan Dirk Jansen [2].

[1]EWI
Delft University of Technology

[2]CiTG
Delft University of Technology

SPE 10

Single-phase flow, grid size 60 x 220 x 85 grid cells.

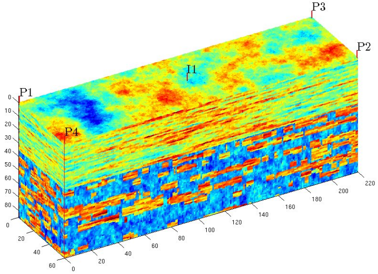

Method	Number of iterations
ICCG	1011
DICCG	2

Table : Number of iterations for the SPE 10 benchmark (85 layers) for the ICCG and DICCG methods, tolerance of 10^{-7}.

Table of Contents

Problem Definition

Reservoir Simulation

Single-phase flow through a porous media [1]

Darcy's law + mass balance equation

$$-\nabla \cdot \left[\frac{\alpha\rho}{\mu}\vec{\mathbf{K}}(\nabla \mathbf{p} - \rho g \nabla d)\right] + \alpha\rho\phi c_t \frac{\partial \mathbf{p}}{\partial t} - \alpha\rho\mathbf{q} = 0.$$

$$c_t = (c_l + c_r),$$

α a geometric factor

ρ fluid density

μ fluid viscosity

$\mathbf{p}$ pressure

$\vec{\mathbf{K}}$ rock permeability

g gravity

d depth

ϕ rock porosity

$\mathbf{q}$ sources

c_r rock compressibility

c_l liquid compressibility

Problem Definition

Discretization

2D case, isotropic permeability, small rock and fluid compressibilities, uniform reservoir thickness and no gravity forces.

$$-\frac{h}{\mu}\frac{\partial}{\partial x}\left(k\frac{\partial \mathbf{p}}{\partial x}\right)-\frac{h}{\mu}\frac{\partial}{\partial y}\left(k\frac{\partial \mathbf{p}}{\partial y}\right)-\frac{h}{\mu}\frac{\partial}{\partial z}\left(k\frac{\partial \mathbf{p}}{\partial z}\right)+h\phi_0 c_t\frac{\partial \mathbf{p}}{\partial t}-h\mathbf{q}=0.$$

$$\boxed{\mathcal{V}\dot{\mathbf{p}}+\mathcal{T}\mathbf{p}=\mathbf{q}.}$$

$\mathbf{q}$: sources or wells in the reservoir, Peaceman well model, $\mathcal{I}_{well}$ is the well index

$$\mathbf{q}=-\mathcal{I}_{well}(\mathbf{p}-\mathbf{p}_{well})$$

Accumulation matrix

$$\mathcal{V}=Vc_t\phi_0\mathcal{I},$$

$$V=h\Delta x\Delta y\Delta z.$$

Transmissibility matrix

$$\mathcal{T}_{i-\frac{1}{2},j,l}=\frac{\Delta y}{\Delta x\Delta z}\frac{h}{\mu}k_{i-\frac{1}{2},j,l},$$

$$k_{i-\frac{1}{2},j}=\frac{2}{\frac{1}{k_{i-1,j,l}}+\frac{1}{k_{i,j,l}}}.$$

Problem Definition

Incompressible model

$$\mathcal{T}\mathbf{p} = \mathbf{q}.$$

Compressible model

$$\mathcal{V}^{n+1}\frac{(\mathbf{p}^{n+1} - \mathbf{p}^{n})}{\Delta t^{n}} + \mathcal{T}^{n+1}\mathbf{p}^{n+1} = \mathbf{q}^{n+1}.$$

Or:

$$\mathcal{F}(\mathbf{p}^{n+1}; \mathbf{p}^{n}) = 0. \tag{1}$$

Newton-Raphson

Using Newton-Raphson (NR) method, the system for the $(k+1)$-th NR iteration is:

$$\mathcal{J}(\mathbf{p}^k)\delta\mathbf{p}^{k+1} = -\mathcal{F}(\mathbf{p}^k;\mathbf{p}^n), \qquad \mathbf{p}^{k+1} = \mathbf{p}^k + \delta\mathbf{p}^{k+1},$$

where $\mathcal{J}(\mathbf{p}^k) = \frac{\partial\mathcal{F}(\mathbf{p}^k;\mathbf{p}^n)}{\partial\mathbf{p}^k}$ is the Jacobian matrix, and $\delta\mathbf{p}^{k+1}$ is the NR update at iteration step $k+1$.

$$\mathcal{J}(\mathbf{p}^k)\delta\mathbf{p}^{k+1} = \mathbf{b}(\mathbf{p}^k). \tag{2}$$

Conjugate Gradient Method (CG)

Successive approximations to obtain a more accurate solution $\mathbf{x}$ [2]

$$\mathcal{A}\mathbf{x} = \mathbf{b},$$

$$\mathbf{x}^0, \qquad \text{initial guess} \qquad \mathbf{r}^k = \mathbf{b} - \mathcal{A}\mathbf{x}^{k-1}.$$

$$min_{\mathbf{x}^k \in \kappa_k(\mathcal{A}, \mathbf{r}^0)} ||\mathbf{x} - \mathbf{x}^k||_{\mathcal{A}}, \qquad ||\mathbf{x}||_{\mathcal{A}} = \sqrt{\mathbf{x}^T \mathcal{A}\mathbf{x}}.$$

Convergence

$$||\mathbf{x} - \mathbf{x}^k||_{\mathcal{A}} \leq 2||\mathbf{x} - \mathbf{x}^0||_{\mathcal{A}} \left(\frac{\sqrt{\kappa(\mathcal{A})} - 1}{\sqrt{\kappa(\mathcal{A})} + 1} \right)^k.$$

Preconditioning

Improve the spectrum of $\mathcal{A}$.

$$\mathcal{M}^{-1}\mathcal{A}\mathbf{x} = \mathcal{M}^{-1}\mathbf{b}.$$

Convergence

$$||\mathbf{x} - \mathbf{x}^k||_{\mathcal{A}} \leq 2||\mathbf{x} - \mathbf{x}^0||_{\mathcal{A}} \left(\frac{\sqrt{\kappa(\mathcal{M}^{-1}\mathcal{A})} - 1}{\sqrt{\kappa(\mathcal{M}^{-1}\mathcal{A})} + 1} \right)^k, \qquad \kappa(\mathcal{M}^{-1}\mathcal{A}) \leq \kappa(\mathcal{A}).$$

Deflated PCG

DPCG history

- 1987 Nicolaides and Dostal
  First versions of DPCG
- 1999 Vuik, Meijerink, Segal
  DPCG applied to reservoir simulations (Shell)
- 2004 Nabben, Vuik
  Theory and porous media flow
- 2008 Nabben, Tang, Vuik, ...
  Theory comparison: DPCG, MG and Domain Decomposition, bubbly flow

DPCG

DPCG history

- 2008 Nabben Erlangga
  Convection diffusion, Helmholtz, MLK method
- 2010 Jönsthövel, Vuik
  Mechanical problems, parallel computing
- 2014 Nabben, Sheikh, Lahaye, Vuik, Garcia
  MLK/ADEF method Helmholtz equation
- 2016 Diaz, Jansen, Vuik
  Porous media flow, Model Order Reduction (MOR)

DPCG

Deflation

$$\mathcal{P} = \mathcal{I} - \mathcal{A}\mathcal{Q}, \qquad \mathcal{P} \in \mathbb{R}^{n\times n}, \qquad \mathcal{Q} \in \mathbb{R}^{n\times n},$$
$$\mathcal{Q} = \mathcal{Z}\mathcal{E}^{-1}\mathcal{Z}^T, \qquad \mathcal{Z} \in \mathbb{R}^{n\times k}, \qquad \mathcal{E} \in \mathbb{R}^{k\times k},$$
$$\mathcal{E} = \mathcal{Z}^T\mathcal{A}\mathcal{Z} \text{ (Tang 2008, [3])}.$$

Convergence

Deflated system

$$||\mathbf{x} - \mathbf{x}^k||_{\mathcal{A}} \leq 2||\mathbf{x} - \mathbf{x}^0||_{\mathcal{A}} \left(\frac{\sqrt{\kappa_{eff}(\mathcal{P}\mathcal{A})} - 1}{\sqrt{\kappa_{eff}(\mathcal{P}\mathcal{A})} + 1} \right)^k .$$

Deflated and preconditioned system

$$||\mathbf{x} - \mathbf{x}^k||_{\mathcal{A}} \leq 2||\mathbf{x} - \mathbf{x}^0||_{\mathcal{A}} \left(\frac{\sqrt{\kappa_{eff}(\mathcal{M}^{-1}\mathcal{P}\mathcal{A})} - 1}{\sqrt{\kappa_{eff}(\mathcal{M}^{-1}\mathcal{P}\mathcal{A})} + 1} \right)^k .$$

$$\kappa_{eff}(\mathcal{M}^{-1}\mathcal{P}\mathcal{A}) \leq \kappa_{eff}(\mathcal{P}\mathcal{A}) \leq \kappa(\mathcal{A}).$$

Deflation vectors

Recycling deflation (Clemens 2004, [4]).

$$\mathcal{Z} = [\mathbf{x}^1, \mathbf{x}^2, \mathbf{x}^{q-1}],$$

$\mathbf{x}^i$'s are solutions of the system.

Multigrid and multilevel (Tang 2009, [5]).
The matrices $\mathcal{Z}$ and $\mathcal{Z}^T$ are the restriction and prolongation matrices of multigrid methods.

Subdomain deflation (Vuik 1999,[6]).

Deflation Vectors

Model Order Reduction (MOR)

Many modern mathematical models of real-life processes pose challenges when used in numerical simulations, due to complexity and large size.

Model order reduction aims to lower the computational complexity of such problems by a reduction of the model's associated state space dimension or degrees of freedom, an approximation to the original model is computed. (Vuik 2005, [7])

- Proper Orthogonal Decomposition (POD)
- Reduced Basis Method (RBM)
- Principal Component Analysis (PCA)
- Singular Value Decomposition (SVD)

Deflation vectors

Proposal

Use solution of the system with diverse well configurations '*snapshots*' as deflation vectors (Recycling deflation).

Use as deflation vectors the basis obtained from Proper Orthogonal Decomposition (POD).

Proper Orthogonal Decomposition (POD)

POD: find an 'optimal' basis for a given data set (Markovinović 2009 [8], Astrid 2011, [9])

- Get the snapshots

$$\mathcal{X} = [\mathbf{x}_1, \mathbf{x}_2, ..., \mathbf{x}_m].$$

- Form $\mathcal{R}$

$$\mathcal{R} := \frac{1}{m}\mathcal{X}\mathcal{X}^T \equiv \frac{1}{m}\sum_{i=1}^{m} \mathbf{x}_i \mathbf{x}_i^T.$$

- Then

$$\mathbf{\Phi} = [\phi_1, \phi_2, ...\phi_l] \in \mathbb{R}^{n \times l}$$

are the l eigenvectors corresponding to the largest eigenvalues of $\mathcal{R}$ satisfying:

$$\frac{\sum_{j=1}^{l} \lambda_j}{\sum_{j=1}^{m} \lambda_j} \leq \alpha, \qquad 0 < \alpha \leq 1.$$

Lemma 1

Let $\mathcal{A} \in \mathbb{R}^{n \times n}$ be a non-singular matrix, and $\mathbf{x}$ is a solution of:

$$\mathcal{A}\mathbf{x} = \mathbf{b}. \tag{3}$$

Let $\mathbf{x}_i, \mathbf{b}_i \in \mathbb{R}^n$, $i = 1, ..., m$, be vectors linearly independent ($l.i.$) and

$$\mathcal{A}\mathbf{x}_i = \mathbf{b}_i. \tag{4}$$

The following equivalence holds

$$\mathbf{x} = \sum_{i=1}^{m} c_i \mathbf{x}_i \qquad \Leftrightarrow \qquad \mathbf{b} = \sum_{i=1}^{m} c_i \mathbf{b}_i. \tag{5}$$

Lemma 1 (proof)

$$\text{Proof} \Rightarrow \qquad \mathbf{x} = \sum_{i=1}^{m} c_i \mathbf{x}_i \Rightarrow \mathbf{b} = \sum_{i=1}^{m} c_i \mathbf{b}_i. \tag{6}$$

Substituting $\mathbf{x}$ from (6) into $\mathcal{A}\mathbf{x} = \mathbf{b}$ and using the linearity of $\mathcal{A}$ we obtain:

$$\mathcal{A}\mathbf{x} = \sum_{i=1}^{m} c_i \mathcal{A}\mathbf{x}_i = \sum_{i=1}^{m} c_i \mathbf{b}_i = \mathbf{b}. \qquad \text{Similarly for} \Leftarrow \qquad \boxtimes$$

Lemma 2

If the the deflation matrix $\mathcal{Z}$ is constructed with a set of m vectors

$$\mathcal{Z} = \begin{bmatrix} \mathbf{x}_1 & \dots & \dots & \mathbf{x}_m \end{bmatrix}, \tag{7}$$

such that $\mathbf{x} = \sum_{i=1}^{m} c_i \mathbf{x}_i$, with $\mathbf{x}_i$ *l.i.*, then the solution of system (3) is obtained with one iteration of DCG.

Lemma 2 (proof)

Proof.
The relation between $\hat{\mathbf{x}}$ and $\mathbf{x}$ is given by [3]:

$$\mathbf{x} = \mathcal{Q}\mathbf{b} + \mathcal{P}^T\hat{\mathbf{x}}.$$

For the first term $\mathcal{Q}\mathbf{b}$, taking $\mathbf{b} = \sum_{i=1}^{m} c_i\mathbf{b}_i$ we have:

$$\begin{aligned}
\mathcal{Q}\mathbf{b} &= \mathcal{Z}\mathcal{E}^{-1}\mathcal{Z}^T\left(\sum_{i=1}^{m} c_i\mathbf{b}_i\right) = \mathcal{Z}(\mathcal{Z}^T\mathcal{A}\mathcal{Z})^{-1}\mathcal{Z}^T\left(\sum_{i=1}^{m} c_i\mathcal{A}\mathbf{x}_i\right)\\
&= \mathcal{Z}(\mathcal{Z}^T\mathcal{A}\mathcal{Z})^{-1}\mathcal{Z}^T\left(\mathcal{A}\mathbf{x}_1c_1 + \ldots + \mathcal{A}\mathbf{x}_mc_m\right) = \mathcal{Z}(\mathcal{Z}^T\mathcal{A}\mathcal{Z})^{-1}(\mathcal{Z}^T\mathcal{A}\mathcal{Z})\mathbf{c}\\
&= \mathcal{Z}\mathbf{c} = c_1\mathbf{x}_1 + c_2\mathbf{x}_2 + \ldots + c_m\mathbf{x}_m = \sum_{i=1}^{m} c_i\mathbf{x}_i = \mathbf{x}.
\end{aligned}$$

Lemma 2 (proof)

Therefore,

$$\mathbf{x} = \mathcal{Q}\mathbf{b}, \tag{8}$$

is the solution to the original system.
For the second term of the equation, $\mathcal{P}^T\hat{\mathbf{x}}$, we compute the deflated solution $\hat{\mathbf{x}}$.

$$\begin{aligned}
\mathcal{P}\mathcal{A}\hat{\mathbf{x}} &= \mathcal{P}\mathbf{b} \\
\mathcal{A}\mathcal{P}^T\hat{\mathbf{x}} &= (\mathcal{I} - \mathcal{A}\mathcal{Q})\mathbf{b} && \text{using } \mathcal{A}\mathcal{P}^T = \mathcal{P}\mathcal{A} \text{ [3] and definition of } \mathcal{P}, \\
\mathcal{A}\mathcal{P}^T\hat{\mathbf{x}} &= \mathbf{b} - \mathcal{A}\mathcal{Q}\mathbf{b} \\
\mathcal{A}\mathcal{P}^T\hat{\mathbf{x}} &= \mathbf{b} - \mathcal{A}\mathbf{x} = 0 && \text{taking } \mathcal{Q}\mathbf{b} = \mathbf{x} \text{ from above}, \\
\mathcal{P}^T\hat{\mathbf{x}} &= 0 && \text{as } \mathcal{A} \text{ is invertible.}
\end{aligned}$$

Then we have obtained the solution

$$\mathbf{x} = \mathcal{Q}\mathbf{b} + \mathcal{P}^T\hat{\mathbf{x}} = \mathcal{Q}\mathbf{b},$$

in one step of DCG.

Heterogeneous permeability (Neumann and Dirichlet boundary conditions).

The experiments were performed for single-phase flow, with the following characteristics:

$nx = ny = 64$ grid cells.

5 linearly independent snapshots.

System configuration								
Well pressures (bars)					Boundary conditions (bars)			
	$W1$	$W2$	$W3$	$W4$	$P(y=0)$	$P(y=Ly)$	$\frac{\partial P(x=0)}{\partial n}$	$\frac{\partial P(x=Lx)}{\partial n}$
	-5	-5	+5	+5	0	3	0	0
Snapshots								
	$W1$	$W2$	$W3$	$W4$	$P(y=0)$	$P(y=Ly)$	$\frac{\partial P(x=0)}{\partial n}$	$\frac{\partial P(x=Lx)}{\partial n}$
$\mathbf{z}_1$	-5	0	0	0	0	0	0	0
$\mathbf{z}_2$	0	-5	0	0	0	0	0	0
$\mathbf{z}_3$	0	0	-5	0	0	0	0	0
$\mathbf{z}_4$	0	0	0	-5	0	0	0	0
$\mathbf{z}_5$	0	0	0	0	0	3	0	0

Table : Table with the well configuration and boundary conditions of the system and the snapshots used for the Case 1.

Numerical experiments

Heterogeneous permeability (Neumann and Dirichlet boundary conditions).

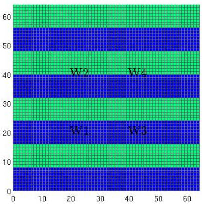

Figure : Heterogeneous permeability, 4 wells.

κ_2 (mD)	10^{-1}	10^{-2}	10^{-3}
ICCG	75	103	110
DICCG	1	1	1

Table : Number of iterations for different contrasts between the permeability of the layers for the ICCG and DICCG methods.

Numerical experiments

Heterogeneous permeability (Neumann boundary conditions).

The experiments were performed for single-phase flow, with the following characteristics:

- $nx = ny = 64$ grid cells.
- Neumann boundary conditions.
- 15 snapshots, 4 linearly independent.
- W1 = W2 = W3 = W4 = -1 bars, W5 = +4 bars.

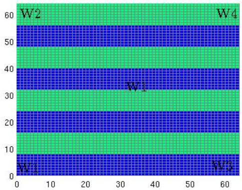

Figure : Heterogeneous permeability layers.

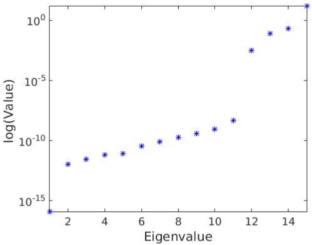

Figure : Eigenvalues of the data snapshot correlation matrix.

σ_2 (mD)	10^{-1}	10^{-2}	10^{-3}
ICCG	90	115	131
$DICCG_4$	1	1	1
$DICCG_{15}$	200*	200*	200*
$DICCG_{POD_4}$	1	1	1

Table : Number of iterations.

Numerical experiments

SPE 10 model

- $60x220x85$ grid cells.
- Neumann boundary conditions.
- 15 snapshots, 4 linearly independent.
- W1 = W2 = W3 = W4 = -1 bars, W5 = +4 bars.

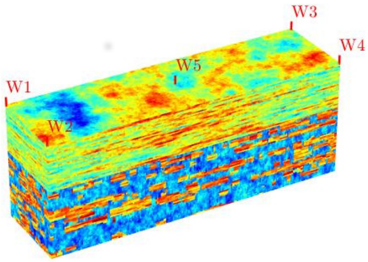

Figure : SPE 10 benchmark, permeability field.

Method	Iterations
ICCG	1011
$DICCG_{15}$	2000*
$DICCG_{4}$	2
$DICCG_{POD_4}$	2

Table : Number of iterations for ICCG and DICCG methods.

Compressible heterogeneous layered problem

35x35 grid cells.

Neumann boundary conditions.

W1 = W2 = W3 = W4 = 100 bars, W5 = 600 bars.

Initial pressure 200 bars.

Contrast between permeability layers of 10^1, 10^2 and 10^3.

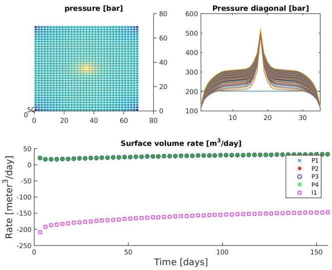

Figure : Solution, contrast between permeability layers of 10^1.

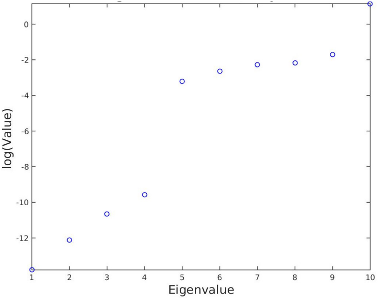

Figure : Eigenvalues of the data snapshot correlation matrix, contrast between permeability layers of 10^1.

Numerical experiments

1^{st} NR Iteration						
$\frac{\sigma_2}{\sigma_1}$	Total ICCG(only)	Method	ICCG Snapshots	DICCG	Total ICCG+DICCG	% of total ICCG(only)
10^1	780	DICCG_{10}	140	42	182	23
	780	DICCG_{POD_6}	140	84	224	29
10^2	624	DICCG_{10}	100	42	142	23
	624	DICCG_{POD_7}	100	42	142	23
10^3	364	DICCG_{10}	20	42	62	17
	364	DICCG_{POD_7}	20	42	62	17

Table : Comparison between the ICCC and DICCG methods of the average number of linear iterations for the first NR iteration for various contrast between permeability layers.

2^{nd} NR Iteration						
$\frac{\sigma_2}{\sigma_1}$	Total ICCG(only)	Method	ICCG Snapshots	DICCG	Total ICCG+DICCG	% of total ICCG(only)
10^1	988	DICCG_{10}	180	78	258	26
	988	DICCG_{POD_6}	180	198	378	38
10^2	832	DICCG_{10}	140	90	230	28
	832	DICCG_{POD_7}	140	154	294	33
10^3	884	DICCG_{10}	110	90	200	23
	884	DICCG_{POD_7}	110	150	260	29

Table : Comparison between the ICCC and DICCG methods of the average number of linear iterations for the second NR iteration for various contrast between permeability layers.

Numerical experiments

Compressible SPE 10 problem

- 60*x*220*x*85 grid cells.
- Neumann boundary conditions.
- W1 = W2 = W3 = W4 = 100 bars, W5 = 600 bars.
- Initial pressure 200 bars.
- Contrast in permeability of $3x10^7$.

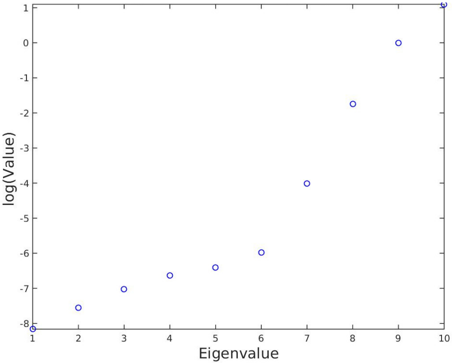

Figure : Eigenvalues of the data snapshot correlation matrix.

Numerical experiments

1^{st} NR Iteration					
Total ICCG(only)	Method	ICCG Snapshots	DICCG	Total ICCG+DICCG	% of total ICCG(only)
10173	$DICCG_{10}$	1770	1134	2904	28
10173	$DICCG_{POD_4}$	1770	1554	3324	32

Table : Total number of linear iterations for the first NR iteration, full SPE 10 benchmark.

2^{nd} NR Iteration					
Total ICCG(only)	Method	ICCG Snapshots	DICCG	Total ICCG+DICCG	% of total ICCG(only)
10231	$DICCG_{10}$	1830	200	2030	20
10231	$DICCG_{POD_4}$	1830	200	2030	20

Table : Total number of linear iterations for the second NR iteration, full SPE 10 benchmark.

Conclusions

- Solution is reached in few (1 or 2) iterations for the DICCG method in the incompressible case.
- A good choice of snapshots takes into account the boundary conditions of the problem.
- The number of iterations of the DICCG method does not depend on the contrast between the coefficients (Heterogeneous permeability example).
- The number of iterations of the ICCG method is reduced up to 80% with the DICCG method in the compressible case.
- Only a limited number of POD basis vectors is necessary to obtain a good speed-up. (for more info see [10, 11])

References I

J.D. Jansen.
A systems description of flow through porous media.
Springer, 2013.

Y. Saad.
Iterative Methods for Sparse Linear Systems.
Society for Industrial and Applied Mathematics Philadelphia, PA, USA. Society for Industrial and Applied Mathematics, 2nd edition, 2003.

J. Tang.
Two-Level Preconditioned Conjugate Gradient Methods with Applications to Bubbly Flow Problems.
PhD thesis, Delft University of Technology, 2008.

M. Clemens; M. Wilke; R. Schuhmann ; T. Weiland.
Subspace projection extrapolation scheme for transient field simulations.
IEEE Transactions on Magnetics, 40(2):934–937, 2004.

Jok Man Tang, Reinhard Nabben, Cornelis Vuik, and Yogi A Erlangga.
Comparison of two-level preconditioners derived from deflation, domain decomposition and multigrid methods.
Journal of scientific computing, 39(3):340–370, 2009.

C. Vuik; A. Segal; and J. A. Meijerink.
An Efficient Preconditioned CG Method for the Solution of a Class of Layered Problems with Extreme Contrasts in the Coefficients.
Journal of Computational Physics, 152:385–403, 1999.

References II

C. Vuik.
Deflation acceleration for CFD problems.
Linear algebra and model order reduction, Model order reduction, coupled problems and optimization from 19 Sep 2005 through 23 Sep 2005, 1:1–1, 2005.

R. Markovinović.
System-Theoretical Model Reduction for Reservoir Simulation and Optimization.
PhD thesis, Delft University of Technology, 2009.

P. Astrid; G. Papaioannou; J. C Vink; J.D. Jansen.
Pressure Preconditioning Using Proper Orthogonal Decomposition.
In *2011 SPE Reservoir Simulation Symposium, The Woodlands, Texas, USA*, pages 21–23, January 2011.

G. B. Diaz Cortes, C. Vuik, and J. D. Jansen.
Physics-based pre-conditioners for large-scale subsurface flow simulation.
Report 16-3, Delft University of Technology, Delft Institute of Applied Mathematics, Delft, 2016.

G.B. Diaz Cortes, C. Vuik, and J.D. Jansen.
Physics-based pre-conditioners for large-scale subsurface flow simulation.
In J.D. Jansen, editor, *ECMOR XV - 15th European Conference on the Mathematics of Oil Recovery, August 29 - September 1, 2016*, pages 1–10, Houten, 2016. EAGE.
DOI: 10.3997/2214-4609.201601801.